Annals of the University of Bucharest (mathematical series)
4 (LXII) (2013), 115–122

In-line phase tomography using nonlinear phase retrieval

Valentina Davidoiu, Bruno Sixou,
Max Langer and Francoise Peyrin

Abstract - With hard X-rays synchrotron beams, phase contrast for in-line phase tomography can be obtained with the measurement of the Fresnel diffraction intensity patterns associated to a phase shift induced by the object. We have studied the resolution of this inverse problem with an iterative nonlinear method. The phase retrieval algorithm was tested for a 3D Shepp-Logan phantom in the presence of noise. The nonlinear scheme outperforms the linear method. Both the high and low frequency ranges of the phase retrieved are improved and the method is less sensitive to noise. In future work, the method will be tested on experimental data. The method is expected to open new perspectives for the study of biological samples.

Key words and phrases : Inverse problems, Phase retrieval, X-ray imaging, X-ray microscopy, In-line phase tomography.

Mathematics Subject Classification (2010) **:** 47J06, 47J25.

1. Introduction

The third-generation of X-rays synchrotron sources allows to obtain coherent hard X-ray beams. The very weak perturbation of the wave front by an object leads to the phase contrast, which can be observed thanks to the coherence properties of the X-ray beam. The Fresnel diffraction framework explains the phase contrast image formation. Large intensity variations associated to the phase shift induced by an object were first reported by Snigirev et al. [19] and by Cloetens et al. [5] at the ESRF (European Synchrotron Radiation Facility). Absorption effects decreases with the energy while the phase measurements may greatly enhance the sensitivity, up to a factor of 10^3. Improving the phase contrast with a smaller absorbed dose in the object is especially interesting for biomedical imaging of soft tissues and microscopy of biopsies. The phase contrast can be measured with techniques based on propagation based imaging [19, 5, 20], interferometry based [2, 14] and analyser-based [4] imaging. The recovery of the phase shift sets a highly ill-posed nonlinear inverse problem. Until recently, the more efficient algorithms were based on a linearization of the relationship between the phase and the intensity. In the literature, two classes of linear algorithms can

be distinguished: some of them use the Transport of Intensity Equation (TIE) [16, 11, 1, 17] based on the linearization for short propagation distances and the others the Contrast Transfer Function (CTF) [5, 21] based on a linearization with respect to the object. An algorithm combining these two methods was proposed by Guigay et al [9], named the Mixed approach. Recently, the phase reconstruction errors have been much decreased by a new approach taking into account the nonlinearity of the inverse problem [7]. The phase and absorption are related to the imaginary and real part of the refractive index by linear line integrals. In a second step, the phase retrieval can thus be coupled to tomography algorithms to reconstruct the refractive index of the object.

The purpose of this work is to use the recently proposed nonlinear phase retrieval method in conjonction with tomographic algorithms to obtain a refractive index map. The reconstruction errors obtained after the phase recovey and tomographic steps will be compared for linear and nonlinear phase retrieval methods. The methods will be tested using the 3D Shepp-Logan phantom in the presence of noise. In this work, we first present the image formation process, the relationships between the phase and the refractive index, and the nonlinear approach for the phase recovery proposed recently. Then we detail the results obtained for the Shepp-Logan phantom.

2. The direct problem

Assuming that the X-ray beam has a high degree of spatial coherence, which is the case for the third-generation synchrotron, the 3D complex refractive index distribution passing through the object usually is written as [3]:

$$n(x, y, z) = 1 - \delta_r(x, y, z) + i\beta(x, y, z) \tag{2.1}$$

where δ_r is the real part of the refractive index and β the imaginary part, for the spatial coordinate (x, y, z). In the following, z denotes the propagation direction of the wave. The coefficients δ and β are wavelength dependent.

Under the hypothesis that the object interacts weakly with the illuminating field, the complex transmission function T of the object can be expressed as:

$$T(\mathbf{x}) = \exp[-B(\mathbf{x}) + i\varphi(\mathbf{x})] = a(\mathbf{x}) \exp[i\varphi(\mathbf{x})] \tag{2.2}$$

where $a(\mathbf{x})$ is the amplitude modulation and $\varphi(\mathbf{x})$ is the phase shift induced by the object. B and φ are related to the real and imaginary part of the complex refractive index by the integral transforms:

$$B(\mathbf{x}) = \frac{2\pi}{\lambda} \int \beta(x, y, z)dz, \qquad \varphi(\mathbf{x}) = -\frac{2\pi}{\lambda} \int \delta_r(x, y, z)dz. \tag{2.3}$$

Thus, once the phase and the absorption are recovered, the real and imaginary parts of the refractive index can be recovered with classical tomographic

reconstruction algorithms. The coherence properties of the incident field enables the measurement of the intensity moving the detector downstream from the object. At a distance D from the object, the Fresnel propagator can be written:

$$P_D(\mathbf{x}) = \frac{1}{i\lambda D} \exp\left(i\frac{\pi}{\lambda D}|\mathbf{x}|^2\right). \tag{2.4}$$

The Fresnel difracted intensity is given by 2D convolution relationship:

$$I_D(\mathbf{x}) = |T(\mathbf{x}) * P_D(\mathbf{x})|^2. \tag{2.5}$$

3. Nonlinear Phase Retrieval Approach

The linear approaches are based on the linearization of the intensity equation (2.5). The most robust to noise is the Mixed approach [13] which is a combination of the Transport of Intensity equation and of the Contrast Transfer Function methods. The phase retrieval problem is ill-posed in the sense that the solution does not depend continuously on the intensity. Hence a stable solution requires regularization techniques. The linear Mixed algorithm uses a classical quadratic Tikhonov regularization [13].

Nonlinear iterative methods have been proposed also for phase retrieval based on propagation based imaging [7, 15]. Thanks to the analytic expressions of the Fréchet derivative of the intensity and of its adjoint, which were given in [7], it was possible to decrease the computation time and to obtain a better convergence. The computation of the phase shift φ is based on the minimization of a regularization functional:

$$J_\alpha(\varphi) = \frac{1}{2}\|I_D(\varphi) - I_\delta\|^2_{L_2(\Omega)} + \frac{\alpha}{2}\|\varphi\|^2_{L_2(\Omega)} \tag{3.1}$$

where I_δ the noisy intensity for the noise level δ, and α a regularization parameter. The iterative formula used to obtain a stationary point of the regularization functional is given by:

$$\varphi_k = \varphi_{k-1} - \tau_{k-1}\{I_D'(\varphi_{k-1})^*[I_D(\varphi_{k-1}) - I_\delta] + \alpha\varphi_{k-1}\}. \tag{3.2}$$

The formula is based on the calculation of the Fréchet derivative and of its adjoint $I_D'(\varphi_k)^*$ [7]. The algorithm is initialized with the solution of the linear problem obtained with the Mixed approach [13]. In the following, the regularization parameter α is chosen with the Morozov principle and then fixed for all the projections directions.

4. Simulations

4.1. Simulation of the image formation

The imaging system was simulated in a deterministic fashion using theoretical values of the refractive index for different materials in the different regions of the Shepp-Logan phantom as in [13]. The 3D Shepp-Logan

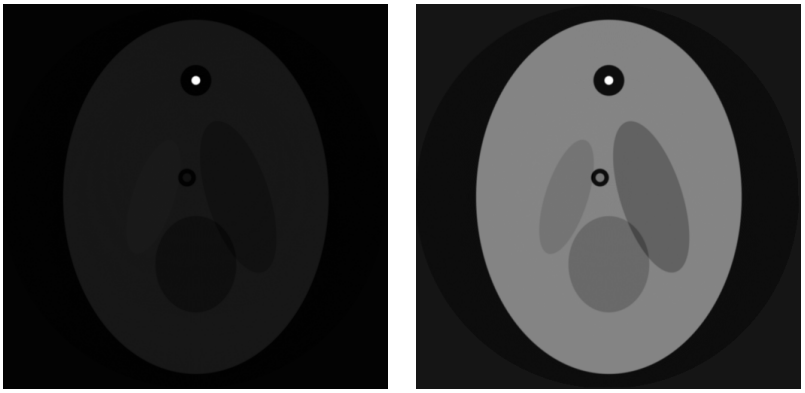

(a) (b)

Figure 1: Central slice of the 3D Shepp-Logan phantom used in the simulations. (a)Absorption index β ($D = 0$ m) (b) and refractive index decrement δ.

is a classical phantom in tomography and consists of a series of ellipsoids on which the projections are based. Two phantoms were defined, one for the absorption coefficient and one for the refractive index decrement displayed in Fig. 1. In our simulations, the X-ray energy was fixed to 24 keV ($\lambda = 0.5166\mathring{A}$) and the pixel size was 1 μm. The intensity images are obtained as the squared modulus of the convolution product with the Fresnel propagator calculated by Fourier transforms, using Eq. 2.5 for three propagation distances $D = [0.035, 0.072, 0.222]$ m. For each distance 1200 angular views were used, sampled on a 2048×2048 grid and down-sampled to 512×512 pixels. The reconstructed tomographic central slices for each distance are displayed in Fig. 2. The three propagation distances are taken into account randomly during the proposed nonlinear algorithm. Simulations were performed with an additive Gaussian noise with zero mean (PP-SNR=12 dB) and without noise. The refractive index reconstructions $\delta(\mathbf{x})$ can be compared directly with the refractive index $\delta^*(\mathbf{x})$ to be recovered using the NMSE (normalized mean square error):

$$NMSE = 100 \times \left(\frac{\sum |\delta(\mathbf{x}) - \delta^*(\mathbf{x})|^2}{\sum |\delta(\mathbf{x})|^2} \right)^{1/2}. \tag{4.1}$$

5. Results

In our tests, we have used the linear Mixed solution as the starting point for the nonlinear method in the phase retrieval step of the index reconstruction. The tomographic reconstruction step is performed using the Filtered Back-Projection (FBP) which is considered as a standard tomographic re-

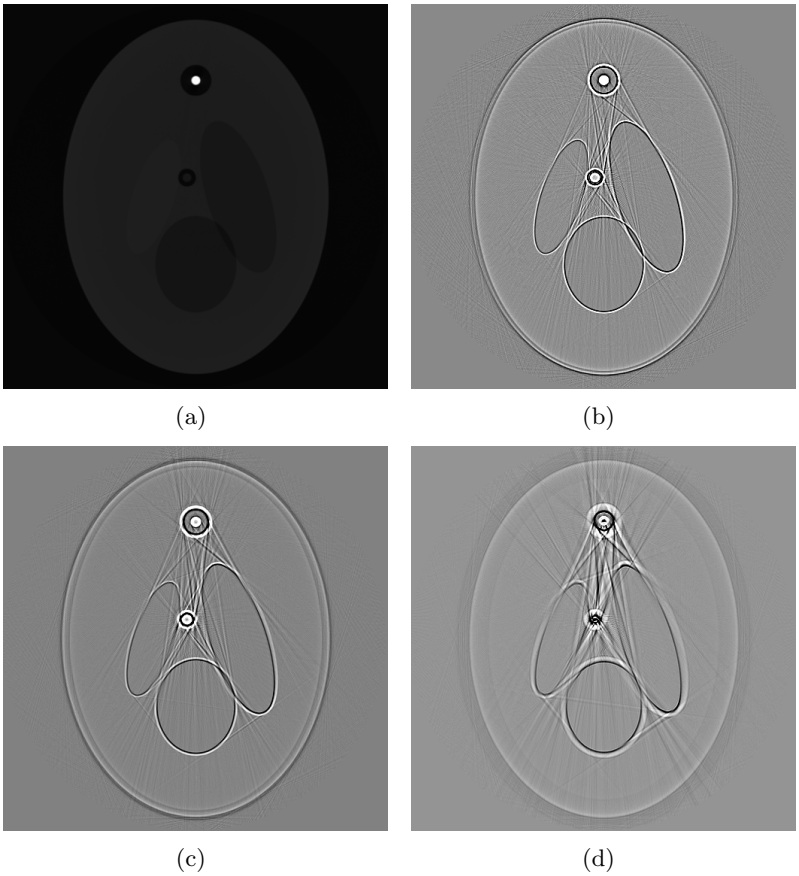

(a) (b)

(c) (d)

Figure 2: Tomographic central slices of the reconstructed refractive index using noiseless data for the Fresnel diffraction pattern at propagation distances (a)($D = 0$ m), (b) $D = 0.035$ m, (c) $D = 0.042$ m and (d) $D = 0.222$ m.

construction algorithm [12]. Fig. 3 shows the reconstructed tomographic central slices of the refractive index phantom using all the distances in the phase retrieval process.

For noiseless data, Fig. 3(a) and Fig. 3(b) displays the reconstructed central slice of the refractive index decrement using the Mixed algorithm and the nonlinear method respectively. For noisy simulated data (PPSNR=12 dB) the central slice of the 3D phantom obtained with the linear method is shown in Fig. 3(c) and the one with the proposed algorithm in Fig. 3(d).

The NMSE for the two compared phase retrieval methods is presented in Table 1, which demonstrates that the proposed nonlinear algorithm gives betters results that the linear Mixed algorithm. The global improvement of the proposed method compared with the linear approach, is 25.43% for the noise-free data and 28.87% for a PPSNR of 12 dB respectively.

Table 1. NMSE(%) values for different algorithms.

PPSNR[dB]	Mixed [NMSE(%)]	Nonlinear [NMSE(%)]
Without noise	30.04%	**22.4**%
12 dB	38.1%	**27.1**%

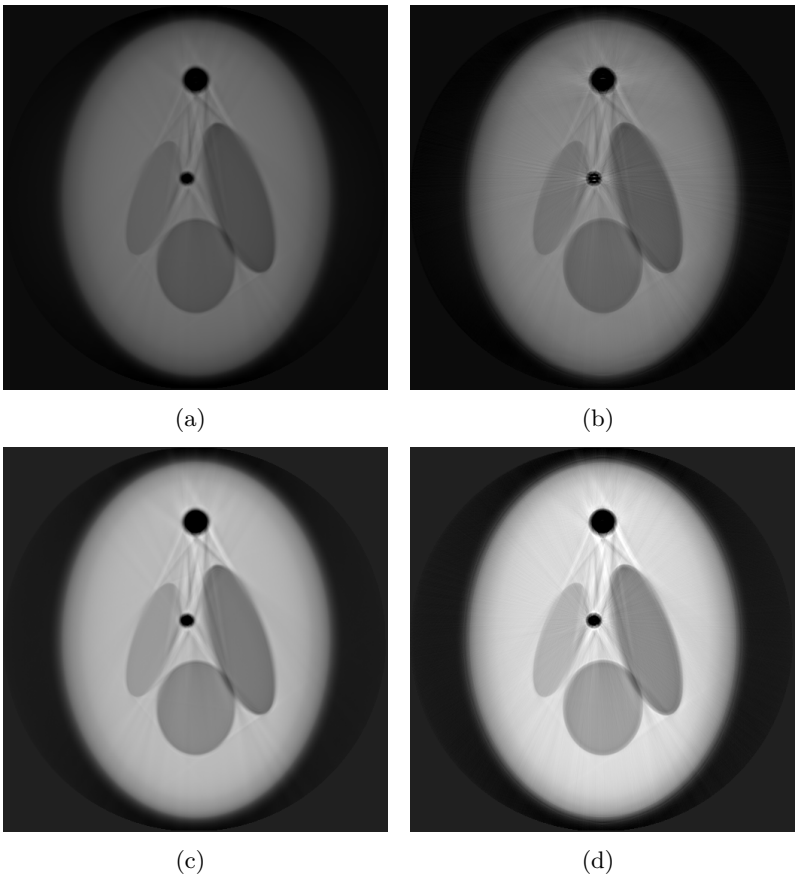

(a) (b) (c) (d)

Figure 3: Central slice of the reconstructed refractive index for the simulated data without noise with (a) Mixed algorithm, (b) the nonlinear method, and with PPSNR=12 dB with (c) Mixed algorithm and (d) the nonlinear method.

Fig. 4(a) displays a comparison of the diagonal profiles obtained without noise for the central slice of the ideal refractive index to be retrieved, and of the refractive index maps obtained with the Mixed or the nonlinear methods. The same profiles are displayed for a PPSNR=12 dB in Fig. 4(b). In these reconstructions is obvious that the phase algorithms are influenced by noise which show typical artifacts at low-frequency. The nonlinear approach yields the most accurate phase map, but rest sensitive to noise.

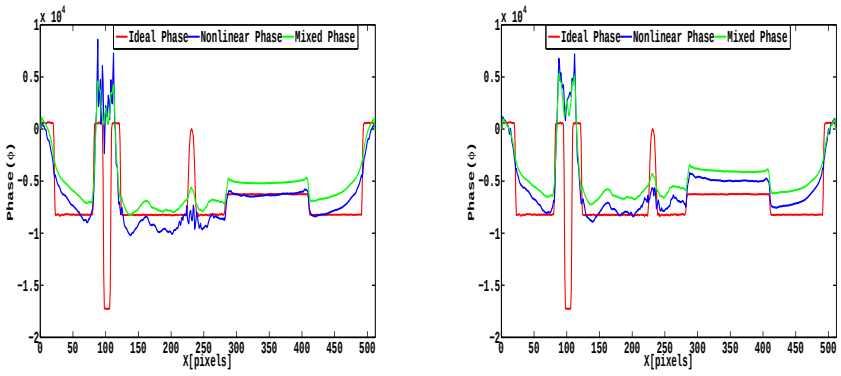

(a) (b)

Figure 4: Diagonal profiles for the central slice of the reconstructed refractive index for the Shepp-Logan phantom obtained with the nonlinear method for Mixed initialization: (a) without noise and (b) with PPSNR=12dB.

6. Conclusion

The reconstruction quality for two phase retrieval methods in in-line phase tomography has been quantitatively evaluated. The phase retrieval algorithms are coupled to tomographic reconstruction schemes to compare the refractive index reconstruction errors. The first approach is the linear Mixed algorithm and the second one is an iterative method based on the Fréchet derivative of the intensity. The reconstructions were compared using a simulated phantom, with and without noise, in terms of NMSE. The nonlinear method gives the best refractive index reconstructions. The method is expected to open new perspectives for the examination of biological samples and will be tested at ESRF on experimental data.

References

[1] M. Beleggia, M.A. Schofield, V.V. Volkov and Y. Zhu, On the transport of intensity technique for phase retrieval, *Ultramicroscopy*, **102** (2004), 37-49 .

[2] U. Bonse and M. Hart, An X-ray interferometer, *Appl. Phys. Lett.,* **6** (1965), 155-156.

[3] M. Born and E. Wolf, *Principles of Optics*, Cambridge University Press, 1997.

[4] D. Chapman, W. Thomlinson, R. E. Johnston, D. Washburn, E. Pisano, N. Gmür, Z. Zhong, R. Menk, F. Arfelli and D. Sayers, Diffraction enhanced x-ray imaging, *Phys. Med. Biol.*, **42** (1997), 2015-2025.

[5] P. Cloetens, R. Barrett, J. Baruchel, J.P. Guigay and M. Schlenker, Phase objects in synchrotron radiation hard X-ray imaging, *J. Phys. D.:Appl. Phys.*, **29** (1996), 133-146.

[6] P. Cloetens, W. Ludwig, J. Baruchel, D. Van Dyck, J. Van Landuyt, J. P. Guigay and M. Schlenker, Holotomography: Quantitative phase tomography with

micrometer resolution using hard synchrotron radiation X rays, *Appl. Phys. Lett.*, **75** (1999), 2912-2914.

[7] V. Davidoiu, B. Sixou, M. Langer and F. Peyrin, Nonlinear phase retrieval based on Frechet derivative, *Opt. Express*, **19** (2011), 22809-22819.

[8] J.R. Fienup, Phase retrieval algorithms: a comparison, *Appl. Opt.*, **21** (1982), 2758-2769.

[9] J. P. Guigay, M. Langer, R. Boistel and P. Cloetens, A mixed contrast transfer and transport of intensity approach for phase retrieval in the Fresnel region, *Opt. Lett.*, **32** (2007), 1617-1619 .

[10] T.E. Gureyev, Composite techniques for phase retrieval in the Fresnel region, *Opt. Commun.*, **220** (2003), 49-58 .

[11] T.E. Gureyev, C. Raven, A. Snigirev, I. Snigireva and S.W. Wilkins, Hard X-ray quantitative non-interferometric phase-contrast microscopy, *J. Phys. D.:Appl. Phys.*, **32** (1999), 563-567 .

[12] A.C. Kak and M. Slaney, *Principles of Computerized Tomographic Imaging*, IEEE Press, New York, 1998.

[13] M. Langer, M. Cloetens, J.P. Guigay and F. Peyrin, Quantitative comparison of direct phase retrieval algorithms in in-line phase tomography, *Med.Phys.*, **35** (2008), 4556-4565.

[14] A. Momose, T. Takeda, Y. Itai and K. Hirano, Phase-contrast X-ray computed tomography for observing biological tissues, *Nat. Med.*, **2** (1996), 473-475.

[15] J. Moosmann, R. Hofmann, A.V. Bronnikov and T. Baumbach, Nonlinear phase retrieval from single-distance radiograph, *Opt.Express*, **18** (2010), 25771-25785.

[16] K.A. Nugent, T.E. Gureyev, D.F. Cookson, D. Paganin and Z. Barnea, Quantitative Phase Imaging Using Hard X Rays, *Phys. Rev. Lett.*, **77** (1996), 2961-2964.

[17] D.M. Paganin, *Coherent X-Ray Optics*, Oxford University Press, New York, 2006.

[18] O. Scherzer, M. Grasmair, H. Grossauer, M. Haltmeier and F. Lenzen, *Variational Methods in Imaging*, Springer Verlag, New York, 2008.

[19] A. Snigirev, I. Snigireva, V. Kohn, S. Kuznetsov and I. Schelokov, On the possibilities of x-ray phase contrast microimaging by coherent high-energy synchrotron radiation, *Rev. Sci. Inst.*, **66** (1995), 5486-5492.

[20] S.W. Wilkins, T.E. Gureyev, D. Gao, A. Pogany and A.W. Stevenson, Phase-contrast imaging using polychromatic hard X-rays, *Nature*, **384** (1996), 335-337.

[21] S. Zabler, P. Cloetens, J.-P. Guigay, J. Baruchel and M. Schlenker, Optimization of phase contrast imaging using hard X-rays, *Rev. Sci. Instrum.*, **76** (2005), 1-7 .

Valentina Davidoiu, Bruno Sixou
CREATIS, CNRS UMR5220; Inserm U630; INSA-Lyon; Université Lyon 1; Université de Lyon, Villeurbanne, France
E-mail: `valentina.davidoiu@creatis.insa-lyon.fr, bruno.sixou@insa-lyon.fr`

Max Langer, Francoise Peyrin
CREATIS, CNRS UMR5220; Inserm U630; INSA-Lyon; Université Lyon 1; Université de Lyon,Villeurbanne, France and
European Synchrotron Radiation Facility, Grenoble, France
E-mail: `max.langer@esrf.fr, eyrin@esrf.fr`